*Journal of Sound and Vibration* (2002) **257**(3), 439–456
doi:10.1006/jsvi.5046, available online at http://www.idealibrary.com on IDEAL®

# AEROELASTIC OSCILLATIONS OF A SEESAW-TYPE OSCILLATOR UNDER STRONG WIND CONDITIONS

H. Lumbantobing and T. I. Haaker

*Department of Applied Mathematical Analysis, Faculty of Information Technology and Systems, Delft University of Technology, PO Box* 5031, 2600 *GA Delft, Netherlands.*
*E-mail: h.lumbantobing@its.tudelft.nl, t.i.haaker@its.tudelft.nl*

(*Received* 19 *July* 2001, *and in final form* 13 *December* 2001)

This paper is concerned with one-degree-of-freedom aeroelastic oscillations of a seesaw-type structure in a steady wind flow. Here it is assumed that strong wind conditions induce nonlinear aeroelastic stiffness forces that are of the same order of magnitude as the structural stiffness forces. As a model equation for the aeroelastic behaviour of the seesaw-type structure, a strongly nonlinear self-excited oscillator is obtained. The bifurcation and the stability of limit cycles for this equation are studied using a special perturbation method. Both the case with linear structural stiffness and the case with nonlinear structural stiffness are studied. For both cases is assumed a general cubic approximation to describe the aerodynamic coefficient. Conditions for the existence, the stability, and the bifurcation of limit cycles are given.



## 1. INTRODUCTION

In this paper the aeroelastic oscillations of a one-degree-of-freedom structure of seesaw-type placed in a steady wind flow with velocity $U$ is considered. A schematic sketch of this seesaw-type oscillator is given in Figure 1. It consists of a rigid bar, holding a cylinder at the right end. On the other end a counter weight is fixed, balancing the cylinder with respect to a hinge axis through the middle of the bar. A torsional spring provides a restoring moment. It is assumed that the cylinder has a uniform cross-section along its axis. If the cylinder has a non-circular cross-section and is exposed to a steady wind flow, perpendicular to the cylinder's axis, self-excited so-called galloping oscillations may arise [1]. Haaker and van der Burgh [2] derived an equation of motion for the seesaw-type oscillator with linear structural stiffness, valid for low flow velocities. The wind forces then act as a perturbation on the *linear* Hamiltonian system that models the unforced oscillations of the seesaw structure. An actual construction of the seesaw-type oscillator was considered in reference [3]. For higher flow velocities, i.e., strong wind, large aerodynamic stiffness forces appear that, when included in the Hamiltonian system, give rise to a perturbed, strongly *nonlinear* Hamiltonian system. In reference [4] a formula was derived for the calculation of the amplitudes of periodic solutions for such a system. Based on this formula the number of periodic solutions, their stability, and also their bifurcation can be studied. Unfortunately, the exact evaluation of that formula is only possible for the simplest cases. For two cases, corresponding to two different symmetric cylinder cross-sections, results concerning the oscillation amplitudes were presented. For one of these cases the results were compared with actual wind tunnel measurements. Contrary to reference [4], here a general class of

0022-460X/02/$35.00 

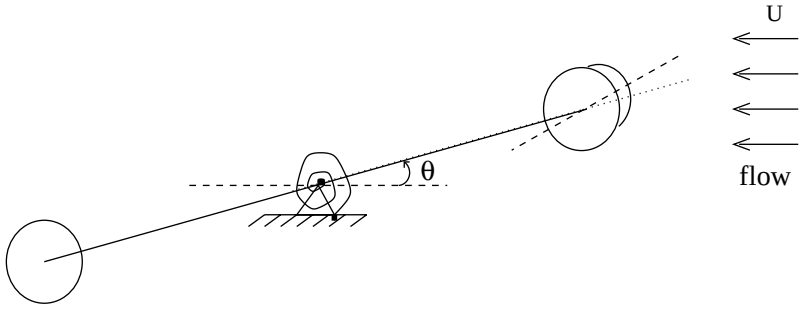


Figure 1. Schematic sketch of the seesaw-type oscillator.

cylinder cross-sections is studied, not necessarily symmetrical. The class studied consists of those cylinder cross-sections for which a cubic approximation of the aerodynamic coefficient curve is appropriate. For two cases a rigorous analytical proof for the existence of a unique stable periodic oscillation is given, based on the monotonicity of certain integral coefficients. Furthermore, strong numerical evidence is given that the monotonicity property also holds for the general case, leading to the conclusion that for this class of cross-sections typically a unique stable periodic oscillation is found. This analysis extends the result of Haaker and Oudheusden [4] to non-symmetric cross-sections. Next, the model studied in references [3, 4] is extended to allow for nonlinear structural stiffness in the equation describing the unforced oscillations. Addition of these nonlinearities leads to new behavior not observed for the case with linear structural stiffness. Again considering the same general class of cross-sections, one finds that there may be two coexisting periodic solutions, one stable and one unstable.

The model equation obtained is a perturbed nonlinear Hamiltonian system. The study of limit cycles for this type of system is generally based on the study of fixed points of a certain Poincaré map. Alternatively, one may study the zeros of the associated distance function, often referred to as the Poincaré–Melnikov function. Doelman and Verhulst [5] applied this method to study the bifurcations of certain strongly nonlinear self-excited oscillators. Van Horssen and Kooij [6] considered the bifurcation of limit cycles for a particular class of quadratic systems with two centers. Iliev and Perko [7] considered the asymmetrically perturbed Duffing equation. These last authors rewrote the Poincaré–Melnikov function as a sum of integral quotients, a method is adopted here. This paper is organized as follows. Section 2 shows the derivation of the model equation for the aeroelastic response of the seesaw-type oscillator. In section 3, the analysis is started by assuming the structural stiffness to be linear. The existence, the stability, and the bifurcation of limit cycles for a general cubic approximation of aerodynamic coefficient curves are considered. The analysis for the case with nonlinear structural stiffness is presented in section 4. For each case phase portraits for a representative numerical example are presented. In section 5, some conclusions will be given.

## 2. DERIVATION OF THE MODEL EQUATION

The result of Haaker and Burgh [2] and Haaker [8], in which the aeroelastic response of the seesaw-type oscillator is derived, is summarized here. The wind forces are modelled using a quasi-steady theory. The angle of rotation described by the bar holding the cylinder is indicated by $\theta$, being positive in counter clockwise direction. The distance from the

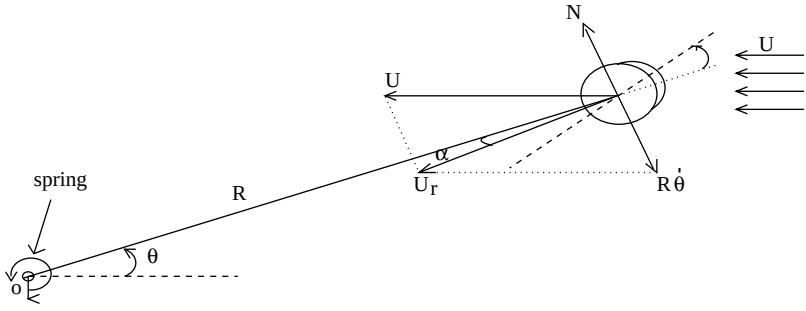


Figure 2. Quasi-steady modelling of seesaw galloping.

cylinder's axis to the pivot O is denoted by $R$, see Figure 2. The aerodynamic moment $M$ exerted on the structure is modelled using the transversal component $N$ of the aerodynamic force exerted on the cylinder. A quasi-steady approach is used to find $N$, that is, it is assumed that $N$ in the dynamic situation is given by the force experienced in the equivalent static situation [8]. Then $N$ is given by $N = \frac{1}{2}\rho l d U_r^2 C_N(\alpha)$ [1], with $\rho$ the density of air, $l$ the length of the cylinder, and $d$ a typical measure for the cylinder cross-section (i.e., diameter for circular section, side-face for rectangular section). $C_N(\alpha)$ is an aerodynamic coefficient curve that depends solely on the shape of the cylinder cross-section and the orientation $\alpha$ toward the experienced flow $U_r$, see Figure 2. This curve may be obtained from static wind tunnel measurements. The orientation, or angle of attack $\alpha$, is in the dynamic situation approximately given by $\alpha = \theta - R\dot{\theta}/U$. Using the aerodynamic coefficient curve $C_N(\alpha)$, the aerodynamic moment is now approximately given by

$$M(\alpha) = \tfrac{1}{2}\,\rho d l R U^2 C_N(\alpha). \tag{1}$$

As a model equation one gets

$$I\ddot{\theta} + c_\theta\dot{\theta} + F(\theta) = \tfrac{1}{2}\,\rho d l R U^2 C_N(\alpha) \tag{2}$$

with

$$F(\theta) = k\theta + \tilde{p}_2\theta^2 + \tilde{p}_3\theta^3. \tag{3}$$

Here $I$ denotes the structural moment of inertia, $c_\theta > 0$ the linear viscous damping coefficient, $U$ the wind velocity, and $F(\theta)$ the restoring structural stiffness force where $\tilde{p}_3 < 0$ is assumed.

Scaling time with $\tau = \omega_\theta t$ where $\omega_\theta^2 = k/I$ and introducing $\varepsilon = \rho d l R^3/(2I)$, $u = U/(\omega_\theta R)$ and $2\xi\varepsilon = c_\theta/(\omega_\theta I)$ yields an equation of motion as follows:

$$\ddot{\theta} + \theta + p_2\theta^2 + p_3\theta^3 = \varepsilon(-2\,\xi\,\dot{\theta} + u^2 C_N(\alpha)). \tag{4}$$

Here $0 < \varepsilon \ll 1$ is a small constant which may be interpreted as a measure for the ratio of displaced air mass to cylinder mass. Note that $u$ is the non-dimensional wind velocity. The assumption used throughout this paper is that $C_N(\alpha)$ cubic, i.e.,

$$C_N(\alpha) = c_1\alpha + c_2\alpha^2 + c_3\alpha^3$$

with $c_1 < 0$ and $c_3 \geqslant 0$.

Substituting for $\alpha$ and $C_N(\alpha)$, equation (4) becomes

$$\ddot{\theta} + (1 - c_1 u^2 \varepsilon)\,\theta + (p_2 - c_2 u^2 \varepsilon)\,\theta^2 + (p_3 - \varepsilon u^2 c_3)\,\theta^3$$

$$= \varepsilon u\left( -\left(\frac{2\xi}{u} + c_1\right)\dot{\theta} + \frac{c_2}{u}\,\dot{\theta}^2 - 2c_2\theta\dot{\theta}^2 - 3c_3\theta^2\dot{\theta} + \frac{3c_3}{u}\,\theta\dot{\theta} - \frac{c_3}{u^2}\,\dot{\theta}^3\right). \quad (5)$$

Assuming a strong wind velocity $u$, i.e., $\varepsilon u^2 = \mathcal{O}(1)$, one may introduce a new $\mathcal{O}(1)$ parameter $\kappa = \varepsilon u^2$ and a new small parameter $\tilde{\varepsilon} = \varepsilon u = \sqrt{\varepsilon\kappa}$ into equation (5) to obtain

$$\ddot{\theta} + (1 - c_1\kappa)\,\theta + (p_2 - c_2\kappa)\,\theta^2 + (p_3 - c_3\kappa)\,\theta^3$$

$$= \tilde{\varepsilon}( - c_1\dot{\theta} - 2\,c_2\,\theta\,\dot{\theta} - 3\,c_3\theta^2\dot{\theta}) + \mathcal{O}(\tilde{\varepsilon}^2). \quad (6)$$

Rescaling $t \to s/\sqrt{1 - c_1\kappa}$, system (6) becomes

$$(1 - c_1\kappa)\,\ddot{\theta} + (1 - c_1\kappa)\,\theta + (p_2 - c_2\kappa)\,\theta^2 + (p_3 - c_3)\,\kappa\,\theta^3$$

$$= \tilde{\varepsilon}( - c_1\sqrt{1 - c_1\kappa}\,\dot{\theta} - 2\,c_2\sqrt{1 - c_1\kappa}\,\theta\,\dot{\theta} - 3\,c_3\sqrt{1 - c_1\kappa}\,\theta^2\dot{\theta}) + \mathcal{O}(\tilde{\varepsilon}^2). \quad (7)$$

Dividing both sides by $(1 - c_1\kappa) > 0$, one gets

$$\ddot{\theta} + \theta + \alpha_{20}\theta^2 + \alpha_{30}\theta^3 = \tilde{\varepsilon}(\alpha_{01}\,\dot{\theta} + \alpha_{11}\theta\,\dot{\theta} + \alpha_{21}\theta^2\dot{\theta}) + \mathcal{O}(\tilde{\varepsilon}^2) \quad (8)$$

with

$$\alpha_{01} = -\frac{c_1}{\sqrt{1 - c_1\kappa}} > 0, \qquad \alpha_{21} = -3\,\frac{c_3}{\sqrt{1 - c_1\kappa}} \leqslant 0,$$

$$\alpha_{11} = -2\,\frac{c_2}{\sqrt{1 - c_1\kappa}}, \qquad \alpha_{20} = \frac{(p_2 - c_2\kappa)}{(1 - c_1\kappa)}.$$

$$\alpha_{30} = \frac{(p_3 - c_3\kappa)}{(1 - c_1\kappa)} \leqslant 0,$$

This is a perturbed Hamiltonian system with Hamiltonian

$$H(\theta, \dot{\theta}) = \tfrac{1}{2}\,\dot{\theta}^2 + \tfrac{1}{2}\,\theta^2 + \tfrac{1}{3}\,\alpha_{20}\theta^3 + \tfrac{1}{4}\,\alpha_{30}\theta^4. \quad (9)$$

## 3. ANALYSIS OF THE MODEL EQUATION FOR LINEAR STRUCTURAL STIFFNESS

This section is concerned with the existence, the bifurcation, and the stability of limit cycles for the linear seesaw oscillator, i.e., equation (4) with $p_2 = p_3 = 0$. The analysis is split in three parts.

### 3.1. CUBIC SYMMETRICAL $C_N(\alpha)$ CASE

In this subsection the cylinder's cross-section is assumed to be symmetrical and the symmetry axis is assumed to coincide with the arm holding the cylinder, implying $c_2 = 0$.

System (8) can be written as follows:

$$\ddot{\theta} + \theta + \tilde{\alpha}_{30}\theta^3 = \tilde{\varepsilon}(\alpha_{01}\dot{\theta} + \alpha_{21}\theta^2\dot{\theta}) + \mathcal{O}(\tilde{\varepsilon}^2), \tag{10}$$

where $\tilde{\alpha}_{30} = -[c_3\kappa/(1 - c_1\kappa)] < 0$.

Rescaling $\theta \to c\bar{\theta}$, after neglecting the "bar", and choosing $c = 1/\sqrt{-\tilde{\alpha}_{30}}$, equation (10) becomes

$$\ddot{\theta} + \theta - \theta^3 = \tilde{\varepsilon}\left(\alpha_{01}\dot{\theta} - \frac{\alpha_{21}}{\tilde{\alpha}_{30}}\theta^2\dot{\theta}\right) + \mathcal{O}(\tilde{\varepsilon}^2). \tag{11}$$

This is a perturbed Hamiltonian system with Hamiltonian

$$H(\theta, \dot{\theta}) = \tfrac{1}{2}\dot{\theta}^2 + \tfrac{1}{2}\theta^2 - \tfrac{1}{4}\theta^4. \tag{12}$$

Letting $\theta = \theta_1$ and $\dot{\theta} = \theta_2$ one gets

$$\begin{aligned} \dot{\theta}_1 &= \theta_2, \\ \dot{\theta}_2 &= -\theta_1 + \theta_1^3 + \tilde{\varepsilon}\left(\alpha_{01}\theta_2 - \frac{\alpha_{21}}{\tilde{\alpha}_{30}}\theta_1^2\theta_2\right) + \mathcal{O}(\tilde{\varepsilon}^2). \end{aligned} \tag{13}$$

The critical points of the unperturbed system are $(0, 0)$ and $(\pm 1, 0)$. Note that $(0, 0)$ is a center point and $(\pm 1, 0)$ are saddle points. One observes that for each $h$ with $0 < h < h_{max}$, the equation $H(\theta, \dot{\theta}) = h$ represents a periodic orbit $\gamma_h$ surrounding the center point $(0, 0)$. The periodic orbits are bounded by two heteroclinic orbits, connecting the two saddle points, obtained from $H(\theta, \dot{\theta}) = h_{max} = \frac{1}{4}$. In order to determine the number of limit cycles of equation (13) one can use Pontryagin's method for perturbed Hamiltonian systems, described, e.g., in Theorem 78 of Andronov *et al.* [9]. This (first order) perturbation theorem shows that precisely one structurally stable limit cycle is bifurcated out of the periodic orbit $\gamma(h_0)$ of unperturbed system (13) if the Poincaré–Melnikov function $I(h)$, given by

$$I(h) = \oint_{\gamma_h}\left(\alpha_{01}\dot{\theta} - \frac{\alpha_{21}}{\tilde{\alpha}_{30}}\theta^2\dot{\theta}\right)\mathrm{d}\theta, \tag{14}$$

has a simple zero at $h = h_0$, that is, $I(h_0) = 0$ and $(\mathrm{d}I/\mathrm{d}h)(h_0) < 0$. One can write the Poincaré–Melnikov function using an integral quotient as follows:

$$\begin{aligned} I(h) &= 4\left(\alpha_{01}I_0(h) - \frac{\alpha_{21}}{\tilde{\alpha}_{30}}I_2(h)\right), \\ &= 4\alpha_{01}I_0(h)\left(1 - \frac{\alpha_{21}}{\alpha_{01}\tilde{\alpha}_{30}}\frac{I_2(h)}{I_0(h)}\right), \\ &= 4\alpha_{01}I_0(h)\left(1 - \frac{\alpha_{21}}{\alpha_{01}\tilde{\alpha}_{30}}Q_{20}(h)\right), \end{aligned}$$

where $I_0(h) = \int_0^{\theta(h)}\dot{\theta}\,\mathrm{d}\theta$, $I_2(h) = \int_0^{\theta(h)}\theta^2\dot{\theta}\,\mathrm{d}\theta$, $\dot{\theta} = \sqrt{G(\theta)}$ with $G(\theta) = 2h - \theta^2 + \frac{1}{2}\theta^4$, $Q_{20}(h) = I_2(h)/I_0(h)$, and the upper boundary of the integrals, $\theta(h)$, is the smallest positive zero of $G(\theta)$.

In Appendix A it is shown that $Q_{20}(h)$ is a strictly increasing function in $h$. The function $I(h)$ has at most one zero depending on the sign of $\alpha_{21}/(\alpha_{01}\tilde{\alpha}_{30})$. This means that there is at most one limit cycle [10]. Now consider the existence of this limit cycle. Notice that $Q_{20}(0) = 0$, $Q_{20}(h_{max}) = \frac{1}{5}$, and $I(h) = 0$ if and only if $Q_{20}(h) = (\alpha_{01}\tilde{\alpha}_{30})/\alpha_{21} = c_1\kappa/(3c_1\kappa - 3)$. Then one can conclude that the limit cycle exists if and only if

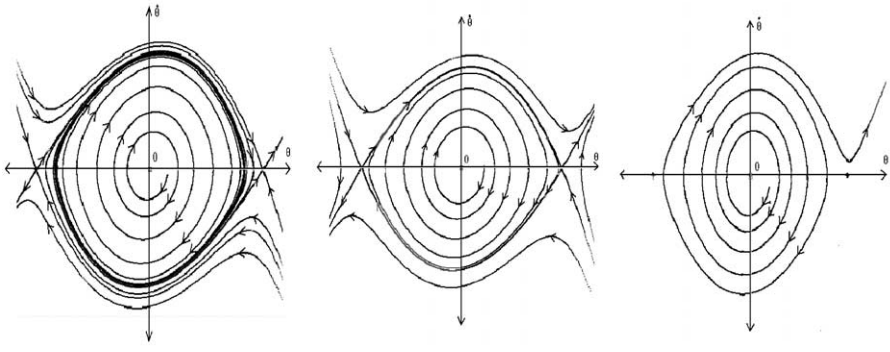

Figure 3. Phase portraits for the cubic symmetrical $C_N(\alpha)$ case for $c_1 = -3$, $c_3 = 1$, and $\varepsilon = 1{\cdot}33 \times 10^{-3}$.

$0 < c_1\kappa/(3c_1\kappa - 3) < \frac{1}{5}$, i.e., $\kappa < -3/(2c_1)$ and a heteroclinic bifurcation occurs for $\kappa = -3/(2c_1)$. The limit cycle is always stable as $\mathrm{d}I/\mathrm{d}h(h) < 0$.

Numerical results for some special values of the parameters are shown in Figure 3. Assuming $\varepsilon = 1{\cdot}33 \times 10^{-3}$ one finds the following results. For $u = 15$ one finds a stable limit cycle. For $u = 19{\cdot}4$, the limit cycle disappears in a heteroclinic bifurcation. For $u = 23$, the system is globally unstable and any initial disturbance leads to an unbounded solution.

### 3.2. QUADRATIC $C_N(\alpha)$ CASE

In this subsection the assumption is made that the cylinder's cross-section is asymmetrical such that a quadratic $C_N(\alpha)$ can be used. Assuming $c_1 < 0$ and $c_2 \neq 0$, system (8) becomes

$$\ddot{\theta} + \theta + \tilde{\alpha}_{20}\theta^2 = \tilde{\varepsilon}(\alpha_{01}\dot{\theta} + \alpha_{11}\theta\dot{\theta}) + \mathcal{O}(\tilde{\varepsilon}^2), \tag{15}$$

where $\tilde{\alpha}_{20} = -c_2\kappa/(1 - c_1\kappa)$.
Rescaling $\theta \to c\bar{\theta}$, after neglecting the "bar", and choosing $c = -1/\tilde{\alpha}_{20}$, equation (15) becomes

$$\ddot{\theta} + \theta - \theta^2 = \tilde{\varepsilon}\left(\alpha_{01}\dot{\theta} - \frac{\alpha_{11}}{\tilde{\alpha}_{20}}\theta\dot{\theta}\right) + \mathcal{O}(\tilde{\varepsilon}^2). \tag{16}$$

This is a perturbed Hamiltonian system with Hamiltonian

$$H(\theta, \dot{\theta}) = \tfrac{1}{2}\dot{\theta}^2 + \tfrac{1}{2}\theta^2 - \tfrac{1}{3}\theta^3. \tag{17}$$

Letting $\theta = \theta_1$ and $\dot{\theta} = \theta_2$ one gets

$$\begin{aligned} \dot{\theta}_1 &= \theta_2, \\ \dot{\theta}_2 &= -\theta_1 + \theta_1^2 + \tilde{\varepsilon}\left(\alpha_{01}\theta_2 - \frac{\alpha_{11}}{\tilde{\alpha}_{20}}\theta_1\theta_2\right) + \mathcal{O}(\tilde{\varepsilon}^2). \end{aligned} \tag{18}$$

The critical points of the unperturbed system are (0, 0) and (1, 0) . Note that (0, 0) is a center point and (1, 0) is a saddle point. Observe that for each $h$ with $0 < h < h_{max}$, the equation $H(\theta, \dot{\theta}) = h$ represents a periodic orbit $\gamma_h$ surrounding the center point (0, 0). The periodic orbits are bounded by a homoclinic orbit, connecting the saddle point to itself, obtained from $H(\theta, \dot{\theta}) = h_{max} = \frac{1}{6}$. Again one can use Pontryagin's method to determine the number

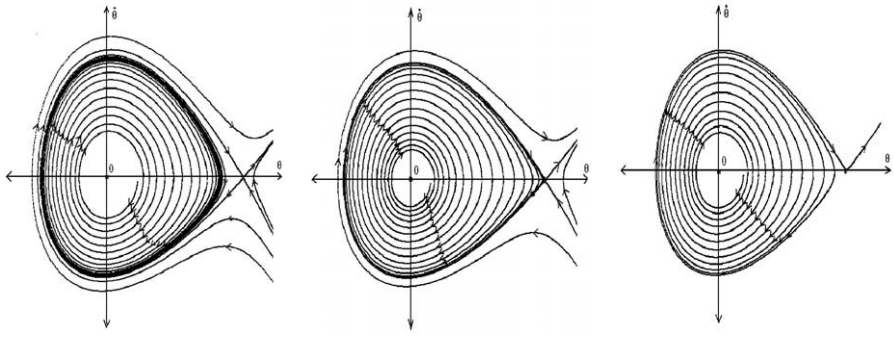

Figure 4. Phase portraits for the quadratic $C_N(\alpha)$ case for $c_1 = -3$, $c_2 = -4$, and $\varepsilon = 1{\cdot}33 \times 10^{-3}$.

and the stability of limit cycles for equation (18). The Poincaré–Melnikov function is given by

$$I(h) = \oint_{\gamma_h} \left( \alpha_{01}\dot{\theta} - \frac{\alpha_{11}}{\tilde{\alpha}_{20}}\theta\dot{\theta} \right) \mathrm{d}\theta. \tag{19}$$

The Poincaré–Melnikov function can be written using an integral quotient as follows:

$$I(h) = 2\alpha_{01} I_0(h) \left( 1 - \frac{\alpha_{11}}{\alpha_{01}\tilde{\alpha}_{20}} Q_{10}(h) \right), \tag{20}$$

where $I_0(h) = \int_{\theta_0(h)}^{\theta_1(h)} \dot{\theta}\, \mathrm{d}\theta$, $I_1(h) = \int_{\theta_0(h)}^{\theta_1(h)} \theta\dot{\theta}\, \mathrm{d}\theta$, $\dot{\theta} = \sqrt{G(\theta)}$ with $G(\theta) = (2h - \theta^2 + \frac{2}{3}\theta^3)$, $Q_{10}(h) = I_1(h)/I_0(h)$, and the boundaries of the integrals, $\theta_0(h)$ and $\theta_1(h)$, are the negative root and the smallest positive root of $G(\theta)$, respectively.

In Appendix A it is shown that $Q_{10}(h)$ is a strictly increasing function in $h$. The function $I(h)$ has at most one zero depending on the sign of $\alpha_{11}/(\alpha_{01}\tilde{\alpha}_{20})$. This means that the system has at most one limit cycle. Now consider the existence of this limit cycle. Notice that $Q_{10}(0) = 0$, $Q_{10}(h_{max}) = \frac{1}{7}$, and $I(h) = 0$ if and only if $Q_{10}(h) = (\alpha_{01}\tilde{\alpha}_{20})/\alpha_{11} = c_1\kappa/(2c_1\kappa - 2)$. Then one can conclude that the limit cycle exists if and only if $0 < c_1\kappa/(2c_2\kappa - 2) < \frac{1}{7}$, i.e., $\kappa < -2/(5c_1)$ and a homoclinic bifurcation occurs for $\kappa = -2/(5c_1)$. The limit cycle is always stable as $(\mathrm{d}I/\mathrm{d}h)(h) < 0$. Numerical results for some special values of the parameters are given in Figure 4. Assuming $\varepsilon = 1{\cdot}33 \times 10^{-3}$ one finds the following results. For $u = 8{\cdot}7$ there is a stable limit cycle. For $u = 10$ the limit cycle disappears in a homoclinic bifurcation. For $u = 10{\cdot}3$ the system is globally unstable and any initial disturbance leads to an unbounded solution.

### 3.3. GENERAL CUBIC $C_N(\alpha)$ CASE

Consider the general cubic approximation for $C_N(\alpha)$ with $c_1 < 0$ and $c_3 > 0$. Rescaling $\theta \to c\bar{\theta}$, neglecting the "bar", and choosing $c = -1/\tilde{\alpha}_{20}$, system (8) becomes

$$\ddot{\theta} + \theta - \theta^2 + \eta\theta^3 = \tilde{\varepsilon}\alpha_{01}(\dot{\theta} + \beta\theta\dot{\theta} + \gamma\theta^2\dot{\theta}) + \mathcal{O}(\tilde{\varepsilon}^2), \tag{21}$$

where $\eta = \tilde{\alpha}_{30}/\tilde{\alpha}_{20}^2 < 0$, $\beta = -\alpha_{11}/(\alpha_{01}\tilde{\alpha}_{20}) < 0$, and $\gamma = \alpha_{21}/(\alpha_{01}\tilde{\alpha}_{20}^2) < 0$.

This is a perturbed Hamiltonian system with Hamiltonian

$$H(\theta, \dot{\theta}, \eta) = \tfrac{1}{2}\dot{\theta}^2 + \tfrac{1}{2}\theta^2 - \tfrac{1}{3}\theta^3 + \tfrac{1}{4}\eta\theta^4. \tag{22}$$

Letting $\theta = \theta_1$ and $\dot{\theta} = \theta_2$, system (21) becomes

$$\begin{aligned} \dot{\theta}_1 &= \theta_2, \\ \dot{\theta}_2 &= -\theta_1 + \theta_1^2 - \eta\theta_1^3 + \tilde{\varepsilon}\alpha_{01}(\theta_2 + \beta\theta_1\theta_2 + \gamma\theta_1^2\theta_2) + \mathcal{O}(\tilde{\varepsilon}^2). \end{aligned} \tag{23}$$

The critical points of the unperturbed system are (0, 0) and $((1 \pm \sqrt{1-4\eta})/(2\eta), 0)$. Note that (0, 0) is a center point and $((1 \pm \sqrt{1-4\eta})/(2\eta), 0)$ are saddle points. One observes that for each $h$ with $0 < h < h_{max}$, the equation $H(\theta, \dot{\theta}) = h$ represents a periodic orbit $\gamma_h$, surrounding the center point (0, 0). The periodic orbits are bounded by a homoclinic orbit, connecting the saddle point closest to the center point to itself. The homoclinic orbit is obtained from $H(\theta, \dot{\theta}, \eta) = h_{max} = \frac{1}{96}[(1 + \sqrt{1-4\eta})^2(6\eta - 1 - \sqrt{1-4\eta})]/\eta^3$. The Poincaré–Melnikov function is given by

$$I(h, \eta) = \alpha_{01} \oint_{\gamma_h} (\dot{\theta} + \beta\theta\dot{\theta} + \gamma\theta^2\dot{\theta})\,\mathrm{d}\theta. \tag{24}$$

The Poincaré–Melnikov function is written using an integral quotient as follows:

$$I(h, \eta) = \alpha_{01}\,(I_0(h, \eta) + \beta I_1(h, \eta) + \gamma\, I_2(h, \eta)) \tag{25}$$

$$= \alpha_{01} I_0(h, \eta)\,(1 + \beta\, Q_{10}(h, \eta) + \gamma\, Q_{20}(h, \eta)), \tag{26}$$

where

$$Q_{10}(h, \eta) = \frac{I_1(h, \eta)}{I_0(h, \eta)},\ Q_{20}(h, \eta) = \frac{I_2(h, \eta)}{I_0(h, \eta)},\ I_0(h, \eta) = \int_{\theta_0(h)}^{\theta_1(h)} \dot{\theta}\,\mathrm{d}\theta,\ I_1(h, \eta) = \int_{\theta_0(h)}^{\theta_1(h)} \theta\dot{\theta}\,\mathrm{d}\theta,$$

$$I_2(h, \eta) = \int_{\theta_0(h)}^{\theta_1(h)} \theta^2\dot{\theta}\,\mathrm{d}\theta,\ \dot{\theta} = \sqrt{G(\theta, \eta)} \quad \text{with } G(\theta, \eta) = (2h - \theta^2 + \tfrac{2}{3}\theta^3 - \eta/2\theta^4),$$

and the boundaries of the integrals, $\theta_0(h)$ and $\theta_1(h)$, are the negative and the positive roots of $G(\theta, \eta)$ closest to the center point, respectively.

Numerically, $Q_{10}(h, \eta)$ and $Q_{20}(h, \eta)$ have been calculated for several values of $\eta$. These numerical results indicate that $(\mathrm{d}Q_{10}/\mathrm{d}h)(h, \eta) > 0$ and $(\mathrm{d}Q_{20}/\mathrm{d}h)(h, \eta) > 0$, see Figure 5. So, based on these numerical results one can conjecture the monotonicity of $Q_{10}(h, \eta)$ and $Q_{20}(h, \eta)$. Following from the signs of parameters $\beta$ and $\gamma$ (both negative), one finds that equation (26) has at most one zero. This means that the system has at most one limit cycle. This limit cycle exists if and only if $I(h_{max}, \eta) < 0$. If $h = h_0$ is a zero of $I(h, \eta)$, one gets $(\mathrm{d}I/\mathrm{d}h)(h_0, \eta) = 2\alpha_{01} I_0(h_0, \eta)(\beta(\mathrm{d}Q_{10}/\mathrm{d}h)(h_0, \eta) + \gamma\,\mathrm{d}Q_{20}/\mathrm{d}h(h_0, \eta)) < 0$. So one can conclude that the limit cycle is always stable.

Numerical results for some special values of the parameters are given in Figure 6. Assuming $\varepsilon = 1{\cdot}33 \times 10^{-3}$ one finds the following results. For $u = 8{\cdot}7$ one obtains a stable limit cycle. For $u = 15{\cdot}4$ the limit cycle disappears in a homoclinic bifurcation. For $u = 17{\cdot}3$ the system is globally unstable and any initial disturbance leads to an unbounded solution.

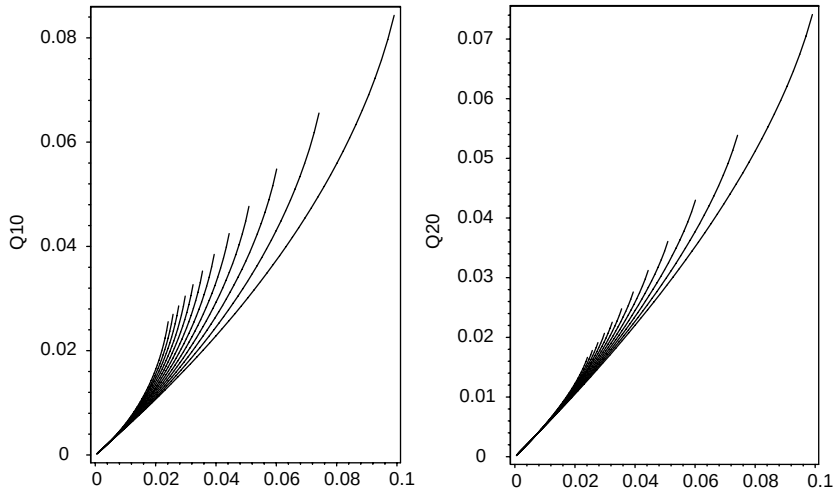


Figure 5. Numerical results of integral quotients $Q_{10}(h, \eta)$ and $Q_{20}(h, \eta)$ for several values of $\eta$.

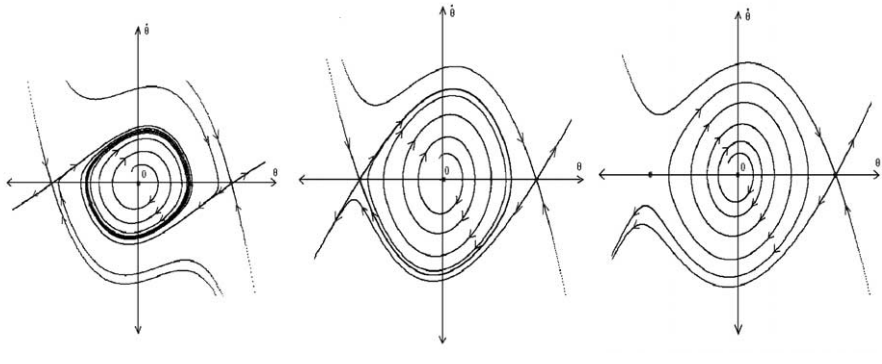

Figure 6. Phase portraits for the cubic non-symmetrical $C_N(\alpha)$ for $c_1 = -3, c_2 = 0{\cdot}25, c_3 = 1$, and $\varepsilon = 1{\cdot}33 \times 10^{-3}$.

## 4. ANALYSIS OF THE MODEL EQUATION FOR NONLINEAR STRUCTURAL STIFFNESS

This section is concerned with the existence, the stability, and the bifurcation of limit cycles for the seesaw-type oscillator with nonlinear stiffness forces, given by equation (8).

Rescaling equation (8) with the transformation $\theta \to c\bar{\theta}$, neglecting the "bar", and choosing $c = -1/\alpha_{20}$ with $\alpha_{20} \neq 0$, one gets

$$\ddot{\theta} + \theta - \theta^2 + \eta\theta^3 = \tilde{\varepsilon}\alpha_{01}\,(\dot{\theta} + \beta\theta\dot{\theta} + \gamma\theta^2\dot{\theta}) + \mathcal{O}(\tilde{\varepsilon}^2), \tag{27}$$

where

$$\eta = \frac{\alpha_{30}}{\alpha_{20}^2} < 0, \quad \beta = \frac{-\alpha_{11}}{\alpha_{01}\,\alpha_{20}} \quad \text{and} \quad \gamma = \frac{\alpha_{21}}{\alpha_{01}\alpha_{20}^2} < 0.$$

This is a perturbed Hamiltonian system with Hamiltonian

$$H(\theta, \dot{\theta}, \eta) = \tfrac{1}{2}\dot{\theta}^2 + \tfrac{1}{2}\theta^2 - \tfrac{1}{3}\theta^3 + \tfrac{1}{4}\eta\theta^4. \tag{28}$$

Note that this equation is the same equation as found for the oscillator with linear stiffness for the cubic non-symmetrical case, equation (21). The only difference is that the sign of the parameter $\beta$ may now be positive.

The existence of bifurcations that create or destroy periodic solutions is considered. First, the existence of homoclinic bifurcations depending on the parameters $\eta$, $\beta$, and $\gamma$ is studied. Recall that a homoclinic bifurcation occurs if the Poincaré–Melnikov function $I(h, \eta)$ is zero for $h = h_{max}$. Using equation (25) one gets the equation

$$I_0(h_{max}, \eta) + \beta I_1(h_{max}, \eta) + \gamma I_2(h_{max}, \eta) = 0. \tag{29}$$

Setting $\gamma$ as a function of the parameters $\eta$ and $\beta$ one obtains

$$\gamma(\eta, \beta) = -\frac{I_1(h_{max}, \eta)}{I_2(h_{max}, \eta)}\beta - \frac{I_0(h_{max}, \eta)}{I_2(h_{max}, \eta)}, \tag{30}$$

where both of $I_1(h_{max}, \eta)/I_2(h_{max}, \eta)$ and $I_0(h_{max}, \eta)/I_2(h_{max}, \eta)$ are positive.

For a fixed value of $\eta$, say $\eta_0$, one obtains a line in the $(\beta, \gamma)$ parameter plane on which the homoclinic bifurcation occurs, see Figure 7,

$$\gamma(\eta_0, \beta) = -\frac{I_1(h_{max}, \eta_0)}{I_2(h_{max}, \eta_0)}\beta - \frac{I_0(h_{max}, \eta_0)}{I_2(h_{max}, \eta_0)}. \tag{31}$$

Another type of bifurcation may occur if the Poincaré–Melnikov function has multiple roots. In particular, a saddle-node bifurcation of periodic solutions appears if both $I(h, \eta)$ and $(\partial I/\partial h)(h, \eta)$ are zero and $(\partial^2 I/\partial h^2)(h, \eta) \neq 0$ for some $(h, \eta) = (h_0, \eta_0)$ , i.e., if

$$I_0(h, \eta) + \beta I_1(h, \eta) + \gamma I_2(h, \eta) = 0, \tag{32}$$

$$\frac{\partial I_0}{\partial h}(h, \eta) + \beta \frac{\partial I_1}{\partial h}(h, \eta) + \gamma \frac{\partial I_2}{\partial h}(h, \eta) = 0, \tag{33}$$

for some $(h, \eta) = (h_0, \eta_0)$. Solving equations (32) and (33) for $\beta$ and $\gamma$ for a fixed value of $\eta$, say $\eta_0$, one obtains a curve in the $(\beta, \gamma)$ parameter plane on which the saddle-node bifurcation occurs (write $J_i = \partial I_i/\partial h$),

$$\begin{pmatrix} \beta(h, \eta_0) \\ \gamma(h, \eta_0) \end{pmatrix} = \frac{-1}{I_1(h, \eta_0)J_2(h, \eta_0) - J_1(h, \eta_0)I_2(h, \eta_0)} \begin{pmatrix} J_2(h, \eta_0) & -I_2(h, \eta_0) \\ -J_1(h, \eta_0) & I_1(h, \eta_0) \end{pmatrix} \begin{pmatrix} I_0(h, \eta_0) \\ J_0(h, \eta_0) \end{pmatrix}. \tag{34}$$

This curve is parameterized by $h$. It terminates on the homoclinic bifurcation line at the point $(\beta_0, \gamma_0) = (\beta(h_{max}, \eta_0), \gamma(h_{max}, \eta_0))$. Note that $(\beta_0, \gamma_0)$ may be viewed as an "organizing center" in the parameter plane in the sense that all different dynamical behavior can be found in a neighborhood of this point. One then obtains the bifurcation diagram as shown in Figure 7. The bifurcation curves divide the $(\beta, \gamma)$ parameter plane into three regions,

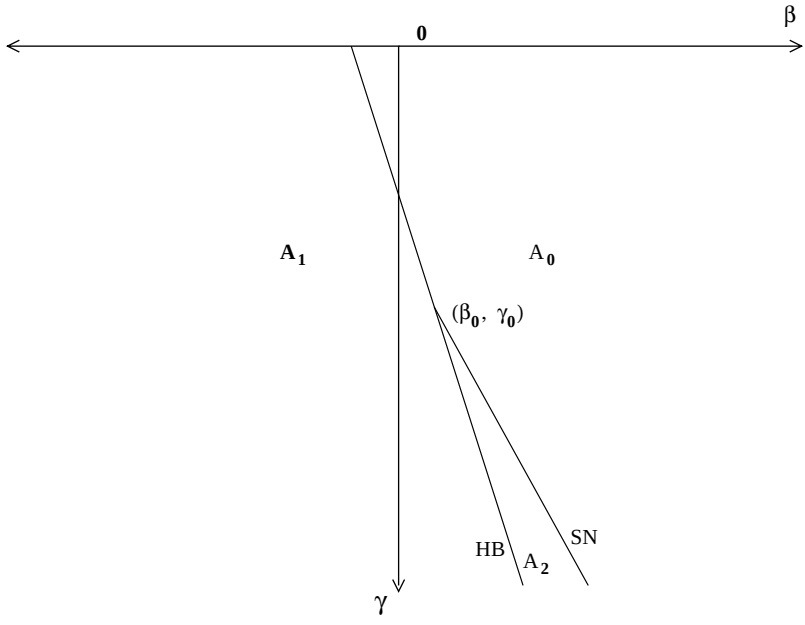


Figure 7. Bifurcation diagram in the $(\beta, \gamma)$ parameter plane. SN, saddle nod bifurcation; HB, homoclinic bifurcation.

that is,

- $A_0$ is the region where one has no limit cycle,
- $A_1$ is the region where one has only one limit cycle,
- $A_2$ is the region where one has two limit cycles.

The number of limit cycles in each region is determined from the number of roots of the Poincaré–Melnikov function in that region, as shown in Figure 8. The case $\beta < 0$ is identical to the situation in section 3.3: below the homoclinic bifurcation line one has a stable limit cycle, above this line no limit cycle is found (see Figure 6 for some phase-portraits for this case).

For $\beta > 0$ the situation is quite different. Starting on the line $\gamma = 0$, one finds readily that $I(h, \eta)$ is positive for $h \in (0, h_{max}]$ and no limit cycle is found. On decreasing $\gamma$ from zero for positive but fixed $\beta$, the Poincaré–Melnikov function remains positive for $h \in (0, h_{max}]$ until either the homoclinic or saddle-node bifurcation curve is reached. In the region $A_0$ therefore no limit cycles are found.

If $\beta$ is chosen such that on decreasing $\gamma$ the homoclinic curve is reached first, then a homoclinic bifurcation occurs in which a stable limit cycle is born. The stability of this limit cycle, $\Gamma(h_0)$, follows from $(\partial I/\partial h)(h_0, \eta_0) < 0$. In the region $A_1$, therefore one has one stable limit cycle.

If $\beta$ is chosen such that on decreasing $\gamma$ the saddle-node curve is reached first, two limit cycles are created in a saddle-node bifurcation. The smaller limit cycle being stable and the larger one being unstable. These limit cycles persist in the region $A_2$ where the Poincaré–Melnikov function has two zeroes. Finally, on reaching the homoclinic curve from region $A_2$, the unstable limit cycle disappears in a homoclinic bifurcation and one enters region $A_1$.

In the three-dimensional $(\eta, \beta, \gamma)$ parameter space, equation (29) defines a surface on which the homoclinic bifurcations occur. Similarly equations (32) and (33) define a surface

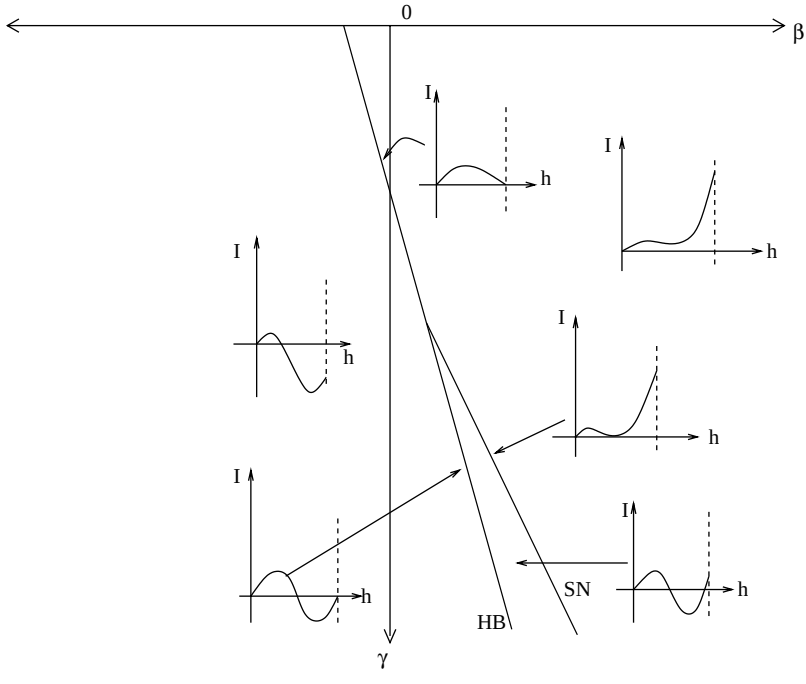


Figure 8. The various shapes of the Poincaré Melnikov functions in the $(\beta, \gamma)$ parameter plane. SN, saddle node bifurcation; HB, homoclinic bifurcation; – – –, maximum value of $h$.

on which the saddle-node bifurcations occur. The intersection of these surfaces defines a curve $(\beta_0(\eta), \gamma_0(\eta))$ consisting of all the points where the saddle-node bifurcation curves end on the homoclinic bifurcation lines. Figure 9(a) shows, for some fixed values of $\eta$, the projection of the homoclinic bifurcation lines on the $(\beta, \gamma)$ bifurcation plane. Figure 9(b) shows, for some fixed values of $\eta$, the projection of the saddle-node bifurcation curves. Also shown is the projection of the curve consisting of termination points $(\beta_0(\eta), \gamma_0(\eta))$.

Now some numerical results are considered for special values of the parameters $\beta$, $\eta$, and $\gamma$. Let $\beta = 400, \eta = -1$ and $\gamma \; -430, \; -487$, and $-530$. Then one obtains Figure 10. Effectively one moves from region $A_0$, through $A_2$ to $A_1$, see Figure 7. For $\gamma = -430$ the system is globally unstable and any initial disturbance leads to an unbounded solution. For $\gamma = -487$ one has two limit cycles, the small limit cycle is stable and the big one is unstable. For $\gamma = -530$ only one stable limit cycle is left.

Finally, the period of oscillation of the limit cycles is considered. Suppose $I(h_0, \eta_0) = 0$, then the limit cycle is to $\mathcal{O}(\varepsilon)$ approximated by the unperturbed orbit $\Gamma(h_0, \eta_0)$. The period of the limit cycle is then approximated to $\mathcal{O}(\varepsilon)$ by the period $T_{\Gamma(h_0, \eta_0)}$ of $\Gamma(h_0, \eta_0)$, given by

$$T_{\Gamma(h_0, \eta_0)} = \int_{\Gamma(h_0, \eta_0)} \frac{\mathrm{d}\theta}{\dot{\theta}} \, \mathrm{d}\theta = \int_{\theta_0(h)}^{\theta_1(h)} \frac{2\mathrm{d}\theta}{\sqrt{2h - \theta^2 + \frac{2}{3}\theta^3 - \frac{1}{2}\eta\,\theta^4}} \, \mathrm{d}\theta, \tag{35}$$

where the boundaries of the integral, $\theta_0(h_0)$ and $\theta_1(h_0)$, are the intersection points of $\Gamma(h_0, \eta_0)$ with the $\theta$-axis. These points follow as the zeroes of $(2h_0 - \theta^2 + \frac{2}{3}\theta - \frac{1}{2}\eta_0\,\theta^4)$, inside the homoclinic loop. Assuming again $\beta = 400$ and $\eta = -1$, the period of the limit cycles is considered when $\gamma$ is varied from $-550$ to $-480$, see Figure 11. Decreasing $\gamma$ from $-480$ one first finds the saddle-node bifurcation for $\gamma = \gamma_{sn} = -485{\cdot}016$ in which the two

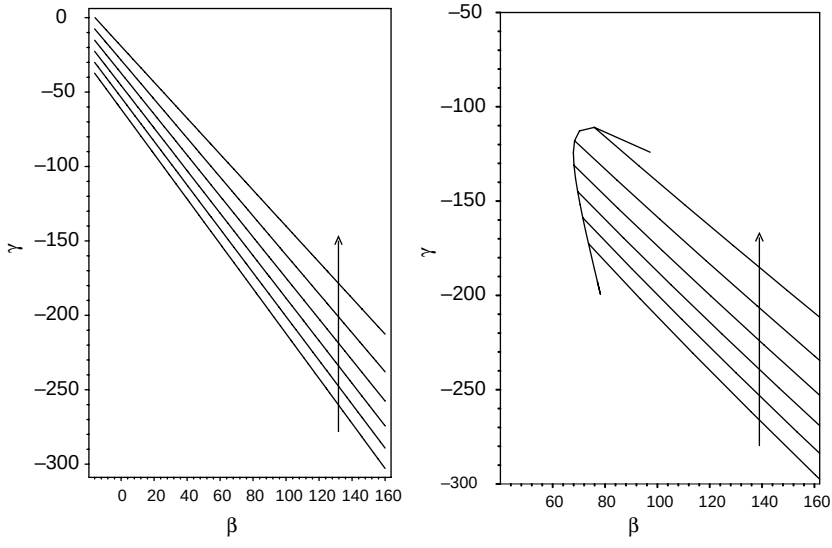


Figure 9. Numerical results for the location of homoclinic and saddle-node bifurcations. The arrow indicates the direction of increasing $\eta$.

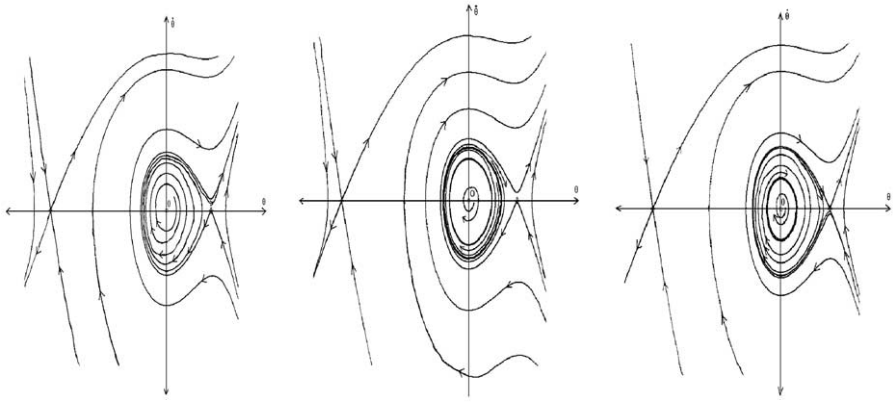

Figure 10. Phase portraits for equation (27) for $\beta = 400, \eta = -1$, and $\tilde{\varepsilon}\alpha_{01} = 0{\cdot}002$.

limit cycles are born. The period of the (shrinking) stable limit cycle decreases when $\gamma$ is further decreased. The period of the (expanding) unstable limit cycle increases when $\gamma$ is further decreased. The period of the unstable limit cycle grows to infinity when it approaches the homoclinic loop $\Gamma(h_{max})$. Then, in the homoclinic bifurcation, for $\gamma = \gamma_{hom} = -523{\cdot}377$, the unstable limit cycle disappears.

## 5. CONCLUSIONS

The aeroelastic response of a single-degree-of-freedom seesaw-type oscillator under strong wind conditions has been considered in this paper. The model equation describing the aeroelastic oscillations is adapted from references [2, 8] and reads

$$\ddot{\theta} + \theta + p_2\theta^2 + p_3\theta^3 = \varepsilon(-2\xi\dot{\theta} + u^2 C_N(\alpha)) \tag{36}$$

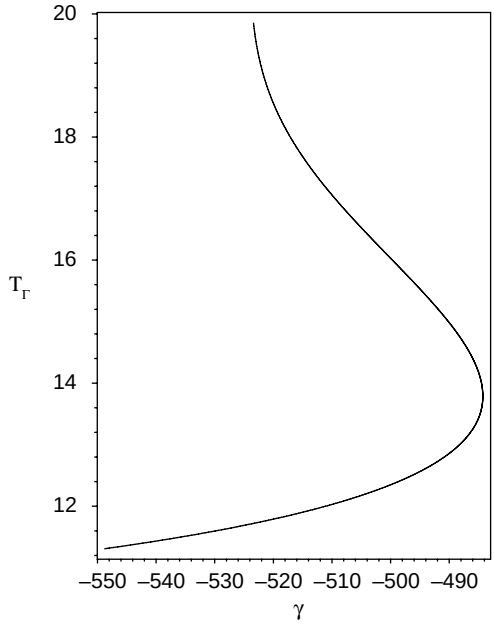


Figure 11. Period of limit cycles for $\eta = -1, \beta = 400$.

with $C_N(\alpha) = c_1\alpha + c_2\alpha^2 + c_3\alpha^3$. In this equation $\theta$ denotes the angle of rotation of the seesaw structure around the hinge axis. It is assumed that $p_3 < 0, c_1 < 0,$ and $c_3 \geqslant 0$. Furthermore, assuming a strong wind velocity $u$, introducing a new parameter $\kappa = \varepsilon u^2 = \mathcal{O}(1)$ and a new small parameter $\tilde{\varepsilon} = \varepsilon u = \sqrt{\varepsilon\kappa}$ to equation (36), one gets a strongly nonlinear system as follows:

$$\ddot{\theta} + \theta + \alpha_{20}\theta^2 + \alpha_{30}\theta^3 = \tilde{\varepsilon}(\alpha_{01}\dot{\theta} + \alpha_{11}\theta\dot{\theta} + \alpha_{21}\theta^2\dot{\theta}) + \mathcal{O}(\tilde{\varepsilon}^2), \tag{37}$$

where $\alpha_{20}$ and $\alpha_{30}$ depend on both structural and aerodynamic force coefficients $\alpha_{01}, \alpha_{11}$, and $\alpha_{21}$ depend on aerodynamic force coefficients and on $\kappa$. Consider first the oscillator with linear structural stiffness, i.e., equation (37) with $p_2 = p_3 = 0$, for three choices of the aerodynamic parameters.

(1) *Case* $c_2 = 0$. Now the equation reads

$$\ddot{\theta} + \theta + \tilde{\alpha}_{30}\theta^3 = \tilde{\varepsilon}(\alpha_{01}\dot{\theta} + \alpha_{21}\theta^2\dot{\theta}) + \mathcal{O}(\tilde{\varepsilon}^2). \tag{38}$$

It is found that a stable limit cycle exists if and only if $\kappa < 3/(-2c_1)$. For $\kappa = 3/(-2c_1)$ a heteroclinic bifurcation destroys the limit cycle, and for $\kappa > 3/-2c_1$ the system is globally unstable. That is, any initial disturbance leads to unbounded solutions.

(2) *Case* $c_3 = 0$. Now the equation reads

$$\ddot{\theta} + \theta + \tilde{\alpha}_{20}\theta^2 = \tilde{\varepsilon}(\alpha_{01}\dot{\theta} + \alpha_{11}\theta\dot{\theta}) + \mathcal{O}(\tilde{\varepsilon}^2). \tag{39}$$

A stable limit cycle exists if and only if $\kappa < 2/(-5c_1)$. For $\kappa = 2/(-5c_1)$ a homoclinic bifurcation destroys the limit cycle, and for $\kappa > 2/(-5c_1)$ the system is globally unstable.

(3) *Case* $c_2 \neq 0, c_3 \neq 0$. Now the equation reads

$$\ddot{\theta} + \theta - \theta^2 + \eta\theta^3 = \tilde{\varepsilon}\alpha_{01}(\dot{\theta} + \beta\theta\dot{\theta} + \gamma\theta^2\dot{\theta}) + \mathcal{O}(\tilde{\varepsilon}^2), \tag{40}$$

where all of the parameters $\beta$, $\eta$, and $\gamma$ are negative.
Based on the numerical analysis one finds at most one limit cycle, which, if it exists, is stable.

Secondly, the seesaw-type oscillator with nonlinear structural stiffness has been considered. Again one obtains equation (40) but now $\beta$ may be positive. One finds that, different from the previous cases, two limit cycles may co-exist. These two limit cycles are shown to be born in a saddle-node bifurcation of periodic solutions. The smaller limit cycle is stable and the larger one is unstable. One obtains regions in the $(\beta, \gamma)$ parameter plane where zero, one, or two limit cycles are found. On the curves separating these regions one finds homoclinic bifurcations or the mentioned saddle-node bifurcations. In the region with no limit cycle the system is globally unstable and any initial disturbance leads to unbounded solutions. Finally, the period of oscillation of the two co-existing limit cycles has been considered for a special case.

## ACKNOWLEDGMENTS

The authors wish to thank Dr. A. H. P. van der Burgh and the referee for careful reading of the manuscript and several valuable comments and suggestions. This research project was sponsored by the Secondary Teacher Development Project (PGSM)—Indonesia with contract No. 6519/0300/Kont-Fel/PGSM and the University of Technology in Delft—The Netherlands. The first author is on leave from Jurusan Pendidikan Matematika, FKIP, Universitas Cenderawasih, Jayapura, Irian Jaya, Indonesia.

## REFERENCES

1. D. Blevins 1990 *Flow-Induced Vibration*. New York: Van Nostrand Reinhold; second edition.
2. I. Haaker and A. H. P. van der Burgh 1994 *SIAM Journal on Applied Mathematics* **54**, 1033–1047. On the dynamics of aeroelastic oscillators with one degree of freedom.
3. W. van Oudheusden 1995 *Nonlinear Dynamics* **8**, 435–451. On the quasi-steady analysis of one-degree-of-freedom galloping with combined translational and rotational effects.
4. I. Haaker and B. W. van Oudheusden 1997 *International Journal of Non-linear Mechanics* **32**, 803–814. One-degree-of-freedom rotational galloping under strong wind conditions.
5. A. Doelman and F. Verhulst 1994 *Mathematical Methods in the Applied Sciences* **17**, 189–207. Bifurcations of strongly non-linear self-excited oscillations.
6. W. T. van Horssen and R. E. Kooij 1994 *Journal of Differential Equations* **114**, 538–569. Bifurcation of limit cycles in a particular class of quadratic systems with two centres.
7. I. D. Iliev and L. M. Perko 1999 *Journal of Differential Equations* **154**, 339–363. Higher order bifurcations of limit cycles.
8. I. Haaker 1996 *Ph.D. Thesis, Department of Applied Analysis, Delft University of Technology, Netherlands*. Quasi-steady modelling and asymptotic analysis of aeroelastic oscillators.
9. A. Andronov, E. A. Leontovich, I. I. Gordon and A. G. Maier 1973 *Theory of Bifurcations of Dynamical Systems on Plane, Israel Program of Scientific Translations, Jerusalem*. New York: Wiley.
10. R. Blows and L. M. Perko 1994 *SIAM Review* **36**, 341–376. Bifurcation of limit cycles from centers and separatrix cycles of planar analytic system.
11. V. Prasolov and Y. Solovyev 1997 *Elliptic Functions and Elliptic Integrals*. Translations of Mathematical Monographs, Vol. 170. USA: American Mathematical Society.

## APPENDIX A

In this Appendix the monotonicity proofs of the integral quotients $Q_{20}(h)$ and $Q_{10}(h)$ of sections 3.1 and 3.2, respectively are considered.

### A.1. PROOF OF THE MONOTONICITY OF $Q_{20}$

Consider the monotonicity of $Q_{20}(h)$. From section 3.1 one knows that $I_0(h) = \int_0^{\theta(h)} R(\theta)\, d\theta$, $I_2(h) = \int_0^{\theta(h)} \theta^2 R(\theta)\, d\theta$, and $Q_{20}(h) = I_2(h)/I_0(h)$ with $R(\theta) = \dot{\theta} = \sqrt{2h - \theta^2 + \frac{1}{2}\theta^4}$ and the upper boundary of the integrals, $\theta(h)$, is the smallest positive root of $R(\theta)$. Integrating by parts in $I_0(h)$ one obtains

$$I_0(h) = \int_0^{\theta(h)} \frac{(\theta^2 - \theta^4)}{R(\theta)}\, d\theta. \tag{A.1}$$

Also

$$I_0(h) = \int_0^{\theta(h)} \frac{(2h - \theta^2 + \frac{1}{2}\theta^4)}{R(\theta)}\, d\theta. \tag{A.2}$$

Similarly, one gets

$$3I_2(h) = \int_0^{\theta(h)} \frac{(\theta^4 - \theta^6)}{R(\theta)}\, d\theta, \tag{A.3}$$

and also

$$I_2(h) = \int_0^{\theta(h)} \frac{(2h\theta^2 - \theta^4 + \frac{1}{2}\theta^6)}{R(\theta)}\, d\theta. \tag{A.4}$$

Write $I_i(h) = \int_0^{\theta(h)} \theta^i R(\theta)\, d\theta$ and $J_i(h) = (dI_i/dh)(h) = \int_0^{\theta(h)} (\theta^i/R(\theta))\, d\theta$, $i = 0, \ldots, 6$.

For simplicity $I_i, J_i$, and $Q_{20}$ will be written instead of $I_i(h), J_i(h)$, and $Q_{20}(h)$ respectively. From their definition it follows that $I_0, I_2, J_2$, and $J_4$ are positive for $h > 0$. Also, since $\theta(h) \leqslant 1$, one knows that $J_0 > J_2$.

Using equations (A.1)–(A.4), $I_0$ and $I_2$ can be expressed in terms of $J_i$ as follows:

$$I_0 = J_2 - J_4, \tag{A.5}$$

$$I_0 = 2hJ_0 - J_2 + \tfrac{1}{2} J_4, \tag{A.6}$$

$$3I_2 = J_4 - J_6, \tag{A.7}$$

$$I_2 = 2hJ_2 - J_4 + \tfrac{1}{2} J_6. \tag{A.8}$$

Combining equations (A.5)–(A.6) one gets $J_4 = \frac{4}{3}(J_2 - hJ_0)$. Using equations (A.5)–(A.8) one obtains

$$15I_0 = 20hJ_0 - 5J_2, \tag{A.9}$$

$$15I_2 = 12hJ_2 - 3J_4. \tag{A.10}$$

Because of $J_4 > 0$ one finds $(J_2 - hJ_0) > 0$ and from equation (A.10) one obtains $(4hJ_0 - J_2) > 0$. A straightforward calculation yields

$$\begin{aligned} 15(J_2I_0 - J_0I_2) &= J_2(20hJ_0 - 5J_2) - J_0(12hJ_2 - 3J_4) \\ &= J_2(4hJ_0 - J_2) + 4(J_0 - J_2)\,(J_2 - hJ_0) \\ &> 0. \end{aligned} \tag{A.11}$$

Consider again the derivative of the integral quotient, i.e.,

$$\frac{\mathrm{d}Q_{20}}{\mathrm{d}h} = \frac{(J_2I_0 - J_0I_2)}{I_0^2}. \tag{A.12}$$

Then from inequality (51) one obtains immediately that $\mathrm{d}Q_{20}/\mathrm{d}h > 0$. This implies that the integral quotient $Q_{20}$ is a strictly increasing function in $h$.

## A.2. PROOF OF THE MONOTONICITY OF $Q_{10}$

Consider now the monotonicity of $Q_{10}(h)$. From section 3.2 one gets that $I_0(h) = \int_{\theta_0(h)}^{\theta_1(h)} R(\theta)\,\mathrm{d}\theta$, $I_1(h) = \int_{\theta_0(h)}^{\theta_1(h)} \theta R(\theta)\,\mathrm{d}\theta$, and $Q_{10}(h) = I_1(h)/I_0(h)$ with $R(\theta) = \dot{\theta} = \sqrt{2h - \theta^2 + 2/3\theta^3}$ and the boundaries of the integrals, $\theta_0(h)$ and $\theta_1(h)$, are the negative root and the smallest positive root of $R(\theta)$, respectively. Integrating by parts in $I_0(h)$ one obtains

$$I_0(h) = \int_{\theta_0(h)}^{\theta_1(h)} \frac{(\theta^2 - \theta^3)}{R(\theta)}\,\mathrm{d}\theta. \tag{A.13}$$

Also

$$I_0(h) = \int_{\theta_0(h)}^{\theta_1(h)} \frac{(2h - \theta^2 + \frac{2}{3}\theta^3)}{R(\theta)}\,\mathrm{d}\theta. \tag{A.14}$$

Similarly, one gets

$$2I_1(h) = \int_{\theta_0(h)}^{\theta_1(h)} \frac{(\theta^3 - \theta^4)}{R(\theta)}\,\mathrm{d}\theta, \tag{A.15}$$

and also

$$I_2(h) = \int_{\theta_0(h)}^{\theta_1(h)} \frac{(2h\theta - \theta^3 + \frac{2}{3}\theta^4)}{R(\theta)}\,\mathrm{d}\theta. \tag{A.16}$$

Again one can write $I_i(h) = \int_{\theta_0(h)}^{\theta_1(h)} \theta^i R(\theta)\mathrm{d}\theta$ and $J_i(h) = \mathrm{d}I_i/\mathrm{d}h(h) = \int_{\theta_0(h)}^{\theta_1(h)} \theta^i/R(\theta)\mathrm{d}\theta$, $i = 0, \ldots, 4$.

Using equations (A.13)–(A.16) one can express $I_0$ and $I_2$ in terms of $J_i$, as follows:

$$I_0 = J_2 - J_3, \tag{A.17}$$

$$I_0 = 2hJ_0 - J_2 + \tfrac{2}{3}J_3, \tag{A.18}$$

$$2I_1 = J_3 - J_4, \tag{A.19}$$

$$I_1 = 2hJ_1 - J_3 + \tfrac{2}{3} J_4. \tag{A.20}$$

Combining equations (A.17) and (A.18) one obtains $J_3 = \frac{6}{5}(J_0 - hJ_0)$. Also, applying a theorem of Legendre [11], on egets $J_1 = J_2$. Using equations (A.17)–(A.20) one obtains

$$5I_0 = 6hJ_0 - J_1, \tag{A.21}$$

$$7I_1 = 6hJ_1 - J_3. \tag{A.22}$$

It follows from their definition that $I_0, I_1,$ and $J_i$ are positive for $h > 0$. Also, since $\theta_0(h) < 0$ and $\theta_1(h) > 0$, one knows that $J_0 - J_1 > 0$. As $J_3 > 0$ also $J_1 - hJ_0 > 0$. Finally, from equation (A.21) one gets $6hJ_0 - J_1 > 0$.

A straightforward calculation now yields

$$\begin{aligned} 35(J_1I_0 - J_0I_1) &= J_1(42hJ_0 - 7J_1) + J_0(6(5h - 1)\, J_1 + 6hJ_0) \\ &= (12hJ_0J_1 - 7J_1^2) + (6J_0J_1 - 6hJ_0^2) \\ &= (6hJ_0 - J_1)\, J_1 + 6(J_0 - J_1)\,(J_1 - hJ_0) \\ &> 0. \end{aligned} \tag{A.23}$$

Consider again the derivative of the integral quotient, i.e.,

$$\frac{\mathrm{d}Q_{10}}{\mathrm{d}h} = \frac{(J_1I_0 - J_0I_1)}{I_0^2}. \tag{A.24}$$

Then from inequality (A.23) one obtains immediately that $(\mathrm{d}Q_{10}/\mathrm{d}h) > 0$. This implies that the integral quotient $Q_{10}$ is a strictly increasing function in $h$.